Real-time three-color reflection holographic interferometer

Jean-Michel Desse[1,*] and Jean-Louis Tribillon[2]

[1]Office National d'Etudes et de Recherches Aérospatiales, 5, Boulevard Paul Painlevé, 9045, Lille, France

[2]Délégation Générale à l'Armement, (DGA/MRIS), bis, Avenue de la porte d'Issy, 75015 Paris Cedex, France

*Corresponding author: Jean-Michel.Desse@onera.fr

A compact real-time three-color reflection holographic interferometer (RCRHI) was developed by Office National d'Etudes et de Recherches Aérospatiales for analyzing high-speed flows. As a classical in-line Lippmann–Denisyuk holographic setup, a reflection panchromatic silver-halide holographic plate is used to simultaneously record three reference holograms. The best results are obtained when the diffraction efficiency of the holographic plate reaches 50% for the three wavelengths used (red-green-blue). For that, problems in gelatin shrinkage due to the hologram treatment had to be solved for the two types of holographic plates used (Slavich and Gentet). This new optical setup was applied to analyze the two-dimensional unsteady wake flow around a circular cylinder at Mach 0.45. Interferograms recorded at a high framing rate exhibit very well saturated colors and high contrast, which eases the quasi-automated interferogram analysis. Finally, the evolution in time of the instantaneous gas density field has been obtained from the analysis of several interferograms covering one period of the phenomenon. In the future, the analysis of three-dimensional flows should be investigated using an optical bench based on RCRHI multidirectional tomography.   © 2009 Optical Society of America

OCIS codes: 090.0090, 090.1705, 090.2880, 090.5694, 120.2880.

1. Introduction

Computational fluid dynamics must be validated by fine measurements in a smaller space or a shorter time, or both at once. This is why Office National d'Etudes et de Recherches Aérospatiales (ONERA) has developed optical methods based on real-time true-color holographic interferometry (RCTHI) using transmission holographic plates [1]. This last technique combines the advantages of differential interferometry with those of monochromatic holographic interferometry. With this, not only small path differences but also large ones can be measured because the interference fringe diagram obtained is colored, very broad, and well contrasted. Also, as opposed to monochromatic holographic interferometry that can provide only relative data, color holographic interferometry generates the achromatic fringe and

also provides absolute data throughout the entire field of observation [2]. But, since transmission holograms are used, the diffraction efficiency of holograms just reaches between 10% and 20%, which limits the quality and the contrast of interferences fringes. On the other hand, if reflection holograms are used, the theoretical diffraction efficiency can reach 100% with a monochromatic light. On ONERA's behalf, the development of RCTHI also offers two important advantages. The first one concerns the analysis of three-dimensional (3D) flows and the second one lies in the comparison with digital color holographic interferometry (DCHI).

In fact, ONERA is looking toward analyzing unsteady 3D flows, and the optical setup to be designed must be based on several crossings of the flow along different view angles. It is very evident that a classical optical setup based on monochromatic holographic interferometry defined, for instance, by Surget [3] for analyzing two-dimensional (2D) flows

cannot be reproduced three or four times. Moreover, as the optical differences to measure are smaller in 3D flows than in the 2D case, it is preferable that each optical ray crosses the phenomena twice in order to increase the sensitivity. Also, to simplify the setup, all the optical pieces have to be located on the same side of the wind tunnel, except the flat mirror, which reflects the light rays back into the test section.

In literature, we can find several authors who analyze 3D flows using multidirectional tomography. Cha and Cha [4] and Yan and Cha [5] present holographic interferometric tomography for limited data reconstruction and exploitation to measure an asymmetric temperature field. Fomin [6] and Fomin *et al.* [7] designed an optical scheme for obtaining specklegrams simultaneously in four directions. Pellicia-Kraft and Watt [8,9] built an interferometric tomography apparatus with six viewing directions from which multidirectional datasets were analyzed following a method of examining spatial coherence. The same approach is taken by researchers developing digital holographic interferometric techniques. Timmerman and Watt [10] developed a dual-reference beam holographic interferometer providing six multiple simultaneous views of a compressible flow. One can also note the optical tomograph using six-view interferometers developed by Joannes *et al.* [11] for the measurement of 3D distribution of temperature in an evaporating liquid. All the measurement techniques yield either the derivative of the refractive index (speckle holography, differential interferometry, or back-oriented Schlieren [12]) or the refractive index itself (holographic interferometry) and, very often, the spatial resolution of the recording camera is very low compared to those given by a holographic plate. As the reconstructed field depends strongly on the measured quantity, on the number of viewing directions, and on the spatial resolution, ONERA wanted to develop a metrological tool having limited viewing directions (three or four) and high spatial resolution, and that would yield the absolute value of the gas density field.

On the other hand, if we make a comparison with digital holographic interferometry, it is true that the CCD resolution and size are not as good as that of holographic plates, but, the digital approach is more accessible and versatile since the time for hologram processing is greatly reduced and treatment is purely numerical. For example, Pedrini *et al.* [13] and Pérez-Lopez *et al.* [14] developed high-speed digital holography with a single wavelength. Recently, Yamaguchi *et al.* [15] proposed phase-shifting digital color holography, where three-color digital holograms were recorded with a 1636×1238 pixel matrix with pixel pitches of $3.9\,\mu m \times 3.9\,\mu m$. They showed the possibility for reconstructing a color amplitude image, but the resolution was degraded since the effective pixel number along each wavelength was 818×619. In 2003, Demoli *et al.* [16] developed a quasi-Fourier off-axis experimental setup using a monochrome CCD sensor with 1008×1018 square pixels, $9\,\mu m \times$

$9\,\mu m$ in size. But, the reference and measurement holograms along the three red-green-blue (RGB) channels are successively recorded. A movie showing convective flows induced by the thermal dissipation in a tank filled with oil was built using the three-color results by applying the subtraction method to the digital holograms. Lastly, ONERA built the first digital three-color holographic interferometer for flow visualization. In this technique, microfringes were generated in the observed field and the recording support (holographic plate) was replaced by a specific Foveon CMOS sensor constituted with three stacked photodiode layers. Interference microfringes produced by the superimposition of three reference waves and three probe waves could be simultaneously recorded on the three spectral bands (RGB) and phase and amplitude images were computed using Fourier transform in delayed time. An application was made in the case of the candle plume [17].

On behalf of color holographic image and panchromatic holographic materials, we can note the recent work of Bjelkhagen and Mirlis [18], who produce highly realistic 3D images. They show that the quality of a color hologram depends on the properties of the recording material, and the demand on a panchromatic material for color holography is described.

2. Description of RCRHI Optical Bench

The optical setup could be named "Denisyuk" because it uses reflection holographic plates as in the classical in-line experiment of Lippmann–Denisyuk. To obtain a very simple setup; all the optical pieces are located on the same side of the wind tunnel, except the flat mirror, which reflects the light rays back into the test section. Because of these considerations, the optical setup based on real-time color reflection holographic interferometry (RCRHI) has been designed. It is presented in Fig. 1. The light source used behind the interferometer is constituted with three different lasers. An argon–krypton laser delivers the red line ($\lambda_1 = 647\,nm$). A green line ($\lambda_2 = 532\,nm$) and a blue line ($\lambda_3 = 457\,nm$) are given by two diode-pumped solid-state lasers. A half-wave plate (HWP) is used to rotate the polarization of the blue line and two dichroic plates (DP) allow the mixing of the three lines. An acousto-optic cell (AOC) diffracts the unwanted lines of the argon–krypton laser in the light mask and does not deviate the three wanted patterns that are generated by three appropriate frequencies. A spatial filter (SF) constituted by a microscope objective lens (20×) and a $25\,\mu m$ pinhole, is located just at the focal distance of the large achromatic lens (AL3) that is set in front of the test section (TS) so that the object under analysis is crossed by a parallel light beam 200 mm in diameter. A flat mirror (LFM) located just behind the test section returns the three beams on the hologram (HP) inserted between the quarter-wave plate (QWP) and the large achromatic lens. The hologram is illuminated on two sides by the three collimated
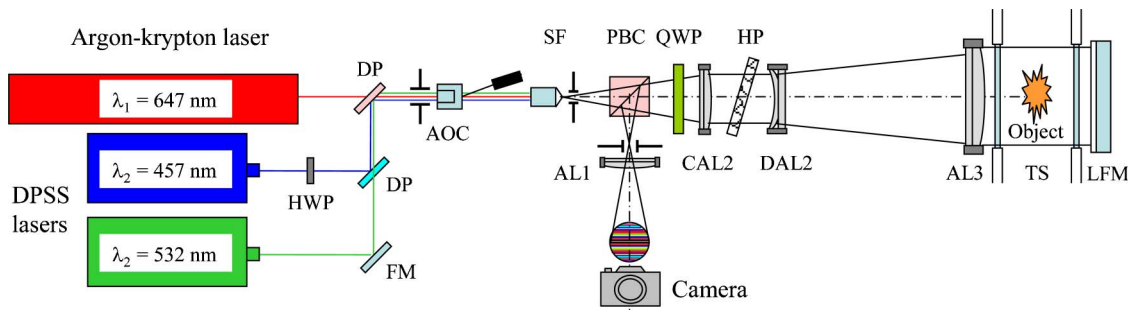
Fig. 1. (Color online) Real-time three-color reflection holographic interferometer.

reference and measurement waves that are formed by the convergent and divergent achromatic (CAL2 and DAL2) lenses. By this arrangement, it is easy to obtain, before the test, a uniform background color or narrowed fringes. In this setup, a polarizing beam splitter cube (PBC) is inserted between the spatial filter and the quarter-wave plate, which transforms the waves' polarization twice (from p parallel to circular and from circular to s parallel) so that, when the rays are returning, the beam splitter cube returns the rays toward the camera. A diaphragm is placed in the focal plane just in front of the camera to filter out any parasitic interference. The interferences fringes produced by the phenomenon under analysis can be directly recorded using a high rotating drum camera. Figure 2 shows photography of the main part of the setup with the nomenclature of the optical pieces.

3. Principle of Real-Time Three-Color Reflection Holographic Interferometry

Figure 3 details how the interferences fringes in the real-time three-color reflection holographic interferometer are generated. First, the holographic plate (HP) is simultaneously illuminated with the three wavelengths. A panchromatic hologram simultaneously records the three interferences fringes produced by the three incident waves and the three waves reflected by the flat mirror (LFM) (first exposure). Then, a hologram is developed and it is reset into the optical bench at the same location. At the second exposure, if the diffraction efficiency of the holographic plate is near 50% for the three lines, 50% of the light is reflected by the hologram (dashed lines).
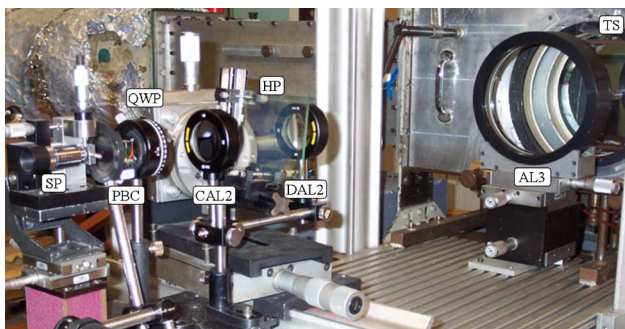

Fig. 2. (Color online) Photography of the mean optical pieces.

If a mask is inserted in front of the test section, one can observe on the screen the three images diffracted by the plate. This operation allows for verifying the quality of the diffracted holograms. When the mask is moved, the other 50% one crosses the test section twice and interferes in real-time with the three reference waves (solid lines). Interferences fringes are not localized because they can be observed from the holographic plate to the camera. If no disturbance exists in the test section, a uniform background color is obtained in the camera. If variation in refractive index exists in the test section, color fringes will be seen on the screen. As the luminous intensities of reference and measurement waves are basically equal, the contrast of color interferences fringes will be maximum.

This optical setup is very simple but it presents an advantage and some inconvenience. The advantage lies in the small number of optical pieces that are used. The reference beams and the measurement beams are collinear and there is just a flat mirror behind the test section. The best holograms are obtained when the holographic plate is placed between the two CAL2 and DAL3 achromatic lenses. The contrast of color interferences fringes depends on the diffraction efficiency of the holographic plate and the color saturation depends on the luminous intensity of the three wavelengths, which can be adjusted with the acousto-optic cell. A main inconvenience rests in the fact that it is not possible to adjust the diffraction efficiency of the holographic plate. It is only fixed by chemical treatment and is a function of gelatin thickness. The unique solution to solve this problem will consist of a specific treatment of the surface of the flat mirror, and this operation implies that the diffraction efficiency of the hologram must already be known.

Finally, the three interferences fringes will exist and can be recorded if the coherence length of the three wavelengths is more than twice the distance between the holographic plate and the flat mirror located just behind the test section. Compared to the setup of transmission holographic interferometry, here it is not possible to adjust the length between the reference and measurement rays.

For information, energy ratios of each wavelength applied at the first exposure are given in Table 1. These values can be compared with tests and results
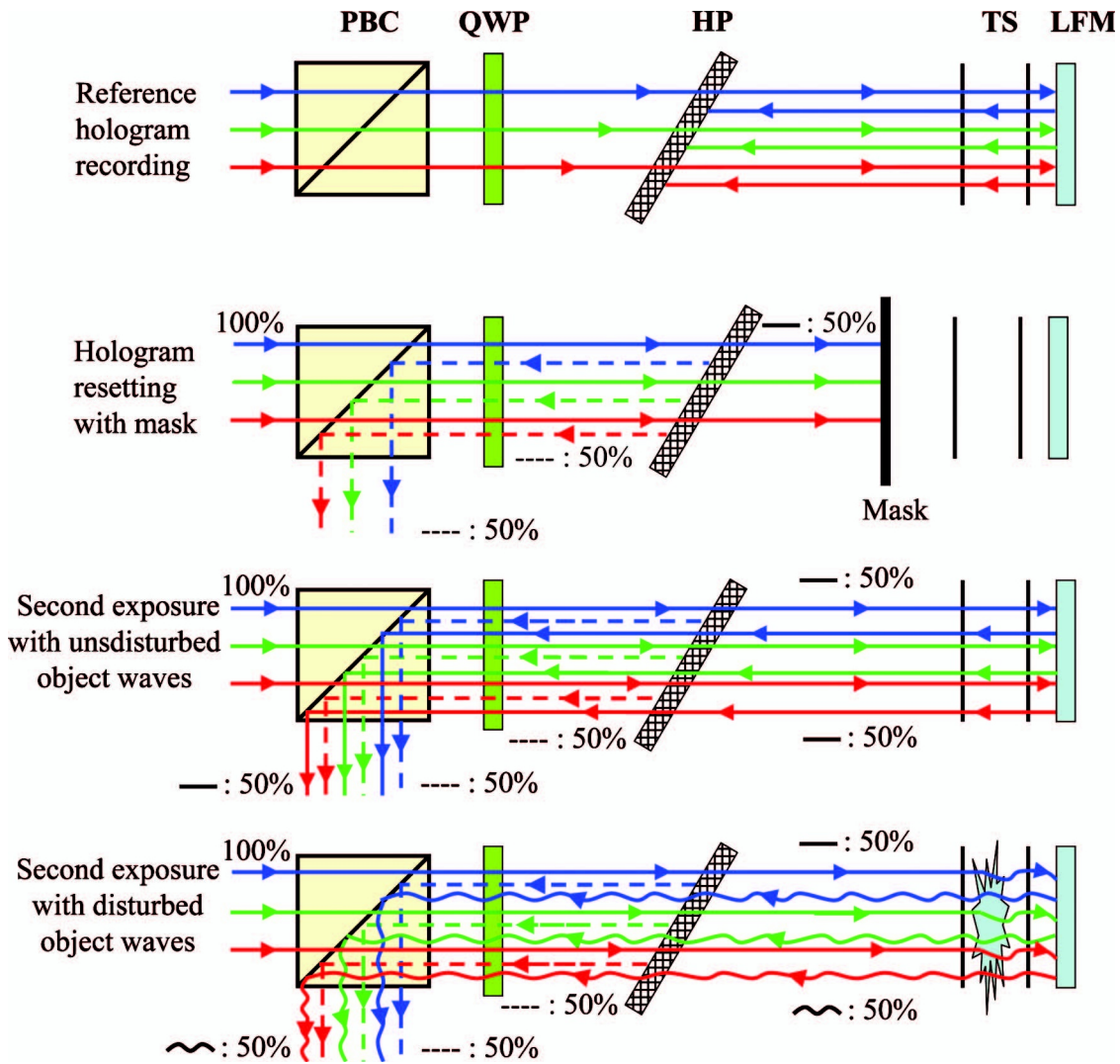
Fig. 3. Principle of color interference fringes in RCDHI setup.

found in Petrova *et al.*[19], who determined the holographic characteristics of panchromatic light-sensitive material for reflective 3D display.

4. Problem of Gelatin Shrinkage

The problem of gelatin shrinkage is widely described in Desse [20]. When the holographic image is recorded by transmission, interference fringes are put down perpendicular to the plate and a small variation in the gelatin thickness caused by the chemical treatment of the hologram does not modify the three interfringe distances. On the other hand, in reflection, interference fringes are recorded parallel to the plate surface and the interfringe distance is very

Table 1. Energy Ratios of Each Wavelength Applied at First Exposure

PFG03c (Slavich)	Ultimate 08 (Gentet)
$1.0 \, 10^{-3} \, \mathrm{J/cm^2}$ at 457 nm	$0.8 \, 10^{-3} \, \mathrm{J/cm^2}$ at 457 nm
$1.3 \, 10^{-3} \, \mathrm{J/cm^2}$ at 532 nm	$0.8 \, 10^{-3} \, \mathrm{J/cm^2}$ at 532 nm
$1.0 \, 10^{-3} \, \mathrm{J/cm^2}$ at 647 nm	$0.8 \, 10^{-3} \, \mathrm{J/cm^2}$ at 647 nm

sensitive to a small variation of the gelatin thickness. For instance, the effects of gelatin contraction when a reflection hologram is recorded with a green wavelength (514 nm) can be evaluated. At restitution, the hologram is illuminated with a white light source (xenon source) at the incidence that the reference wave had at recording. If the gelatin thickness is kept constant ($\Delta e = 0$), the hologram diffracts only the recording wavelength, i.e., for the green hologram, the green wavelength contained in the xenon spectrum. If the gelatin thickness has decreased by 5% ($\Delta e = -0.5 \, \mu$m), the fringe spacing will be proportionally reduced and the diffracted wavelength will be shifted by a quantity equal to

$$\Delta\lambda = \frac{\lambda}{e}\Delta e, \qquad (1)$$

where e is the gelatin layer thickness (about $10 \, \mu$m). The hologram will diffract a wavelength equal to 488.3 nm, corresponding to a blue line. On the other hand, if the gelatin thickness increases by 10%

($\Delta e > 0$), the hologram restituted in white light will diffract a wavelength close to yellow (565.4 nm). On the other, it is well known that the chromatic perceptibility of the eye δl varies with the wavelength. It is defined as being the variation δl between two different wavelengths perceived by the eye at constant luminosity. It is about 1 nm in the green and yellow colors and 6 nm in the blue and red colors, which correspond to relative variations of 0.2% and 1.5%, respectively. For the diffracted color change not to be detected by a human eye, it is mandatory that $\delta l / \lambda$ be less than $\delta \lambda / \lambda$, which implies the variation in gelatin thickness be controlled with an accuracy of less than 0.2%. As the optical technique is based of the knowledge of the true colors diffracted by the hologram, variations of the gelatin thickness are a cause for strong errors in the data analysis. It is for this reason that the gelatin shrinkage problem has to be perfectly mastered. In this experiment, two types of holograms have been tested: Russian plates (PFG03c) from Slavich and French plates (Ultimate 08) from Gentet, typically $10 \, \mu m$ thick. This means that changes in thickness of more than 20 nm are not acceptable.

The diffraction efficiency (DE) of the holographic plates can be evaluated when Russian or French plates are illuminated in white light. For example, Fig. 4 shows how the diffraction efficiency of the Gentet holographic plate is determined from the spectrum of the xenon light source transmitted by the plates. It very easy to see the three hollows corresponding to the part of the white light diffracted by
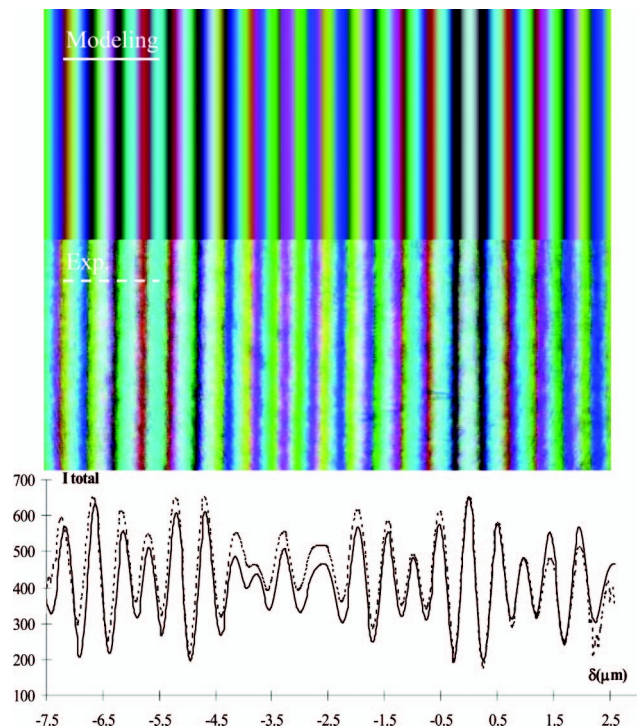

Fig. 5. Comparison between experimental and modeled fringe colors.

the Gentet holographic plate. For each line, the bandwidth in wavelength can be determined when the diffraction efficiency is more than 35%. For the blue line, the acceptable wavelength shift is 8 nm, which corresponds to 9 nm (1.75%) for the green line and
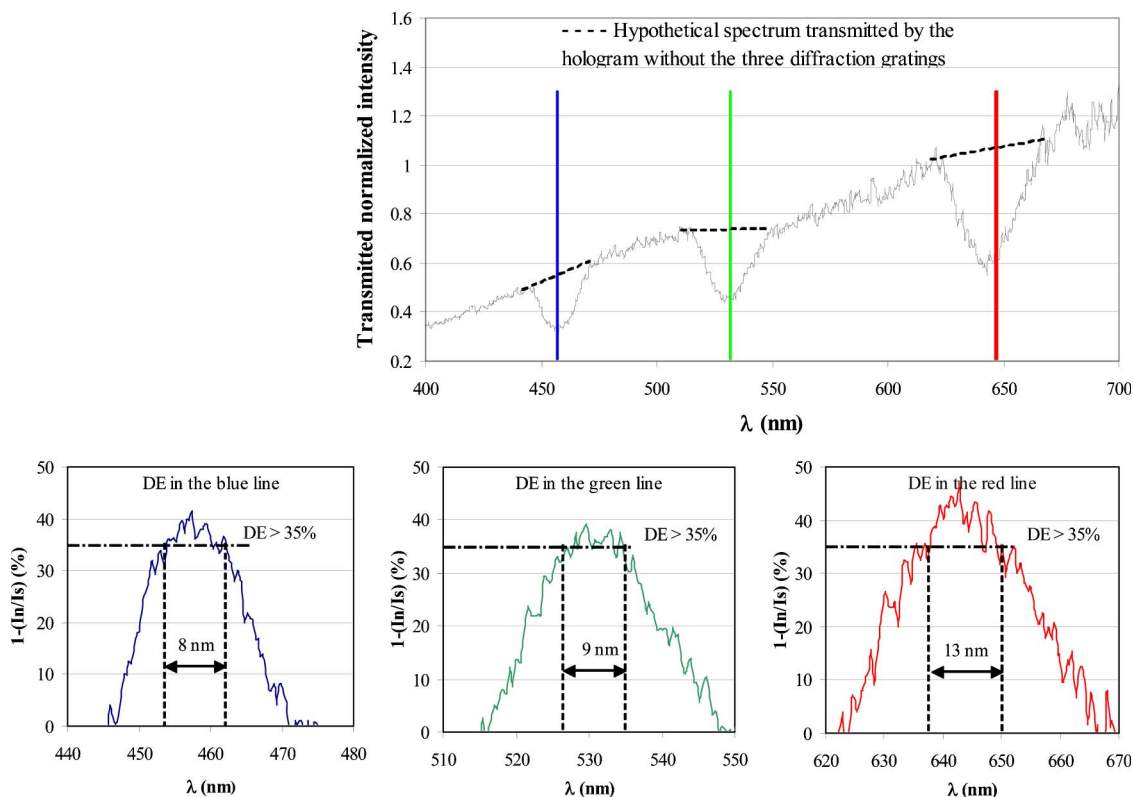

Fig. 4. (Color online) Evaluation of diffraction efficiency of Gentet plate.

13 nm (2%) for the red line. This particularity is very interesting, because the theoretical constraints in the variation of the gelatin thickness (near 0.2%) become larger (about 1.75%) due to the spectral broadening of the transmission curve. As regards the luminous intensity, when the diffraction efficiency of the holographic plate is equal to or more than 35%, the visibility coefficient of interference fringes $((I_{max} - I_{min})/(I_{max} + I_{min}))$ is near 0.21, which means the color interference pattern will be very contrasted.

As regards results previously obtained by ONERA, DCHI and RCRHI can be compared. In RCRHI, a reflection panchromatic holographic plate (7000–10,000 lines/mm in spatial resolution) must be illuminated with a total energy of $600\,\mu J$, and the implementation of the optical setup is not very easy. In DCHI, energy of $1\,\mu J$ is sufficient to illuminate the Foveon sensor (200 lines/mm in resolution). The implementation is easy enough and the phase differ-

ence is entirely estimated with a computer. Concerning the length coherence of the three lasers, it has to be more than 2 m in the RCRHI bench and only several centimeters for DCHI. In RCRHI, about 220 successive frames of the phenomenon can be recorded at a high framing rate (35,000 images/s, with an exposure time of 750 ns for each). Each image has to be digitalized and processed. Also, it is important to obtain a reference hologram of about 50% diffraction efficiency for the three lines. In DCHI, the framing rate is limited to 8 frames/s, full size, and some problems can be encountered with the RGB filters overlapping. But, if another color camera is used, the frame number can be strongly increased.

5. Implementation of the RCRHI in a Wind Tunnel

The RCRHI bench has been implemented in the ONERA transonic wind tunnel. The test section windows are 200 mm in diameter and the unsteady wake flow around a circular cylinder, 20 mm in
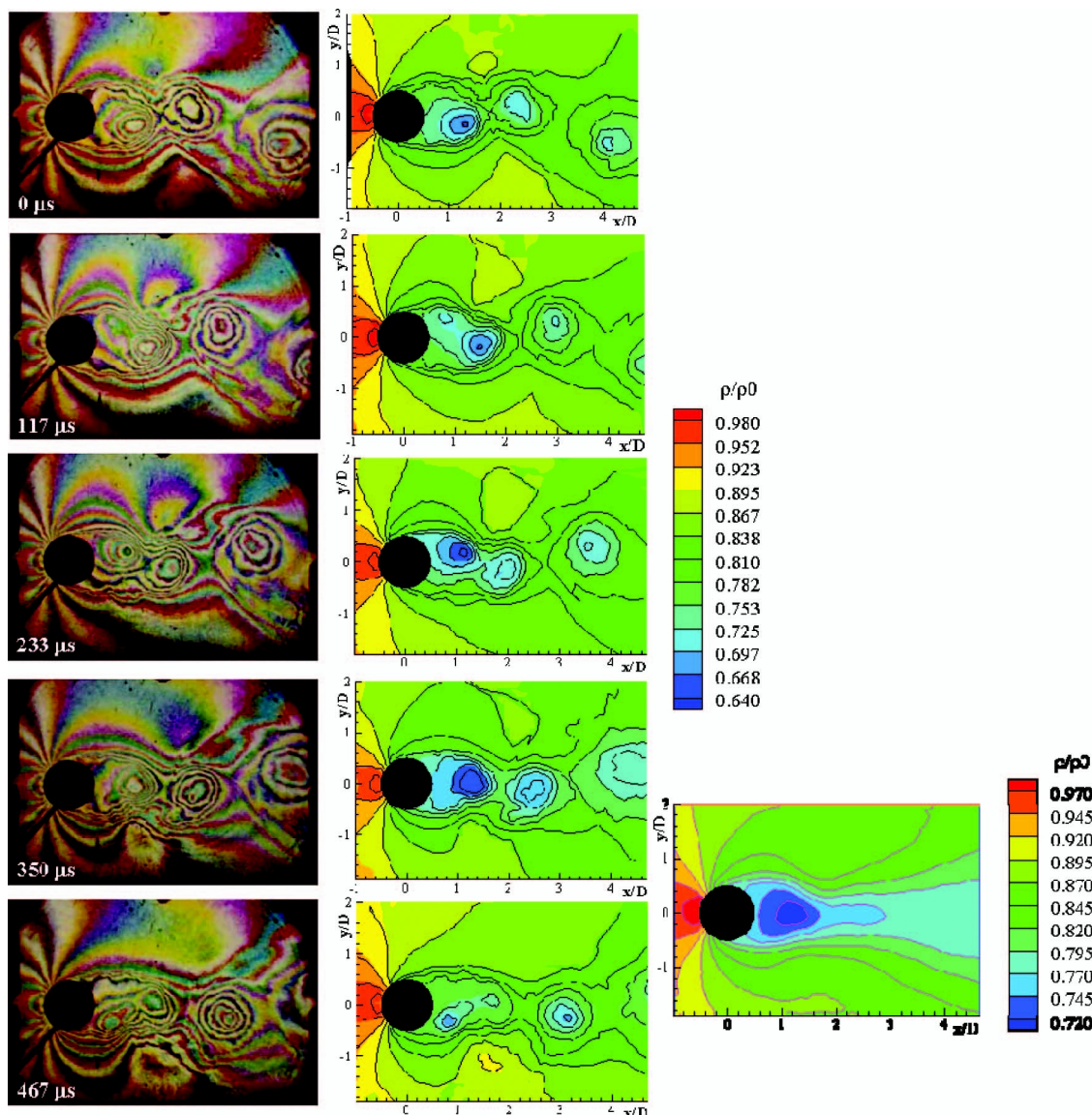

Fig. 6.   Interferogram analysis: instantaneous and average gas density field.

diameter, is under analysis. In this experiment, the infinite Mach number was fixed to 0.45 and the high-speed interferograms were recorded with the rotating drum camera, which is equipped with 400 ASA color film. The time interval between two successive frames is $27\,\mu$s. The time exposure ($750\,$ns) of each interferogram is given by a small window size inside the camera, and the number of recorded interferograms is about 220. The images are $8\,$mm $\times$ $10\,$mm in size and they are digitalized with a SONY 325P video camera through a Matrox image-processing board.

Several movies have been recorded with infinite, circular, and finite fringes. As the optical setup is very sensitive to external vibrations, the uniform background color is difficult to adjust when the wind tunnel is running, but the fringe formation can be observed on the hologram surface, so that it is possible to adjust the uniform background color with the operating wind tunnel.

For analyzing interferograms, ONERA has developed a modeling of fringe color when the optical path difference varies. A comparison between the color of experimental fringes recorded at a high framing rate and the color of fringes computed with the ONERA "MIDI" software is shown in Fig. 5. In modeling, we have to take the spectral characteristics of the luminous light source and the three (RGB) camera filters into account to analytically express the luminous intensity of the interference fringes as a function of the optical path difference. Then, it is possible to reproduce the experimentally visualized colors on the monitor [21]. In this comparison, the transfer function of the holographic plate is not known and cannot be taken into account in the modeling. Nevertheless, the experimental colors exhibit a succession of colors and a white fringe similar to those numerical colors, and they are a little bit more stretched. The relative good agreement between theoretical and experimental fringes gives some assistance to the operator for the interferogram analysis.

Figure 6 shows five of 12 interferograms covering about a period of the phenomenon. They are recorded in infinite fringes. The interferogram colors are well saturated and more contrasted than those obtained in previous experiments performed with transmission holograms [20]. When the background color is uniform, it is very easy to follow the vortices emitted from the upper and lower sides. For instance, if we look at the colors coming out in the vortex cores, we can see that the first vortex emitted from the upper side enters in a formation phase where the gas density decreases in the vortex center. A second phase of dissipation is observed by looking at the last vortex leaving the observed field. This vortex stretches and the gas density increases in the vortex center. Finally, as the technique used is based on holographic interferometry, each color represents a value of the gas density. In analysis, the gas density field was referred to as ρ_0, the stagnation gas density. One can see that the instantaneous gas density var-

ies from 0.64 to 0.98. The average gas density field has been calculated from 12 interferograms. The interferogram number is not very significant, but the obtained field is already symmetrical enough, and the gas density varies from 0.72 to 0.97. Finally, if the color scale of interference patterns is very well known by the user, the image of the interferograms is sufficient to correctly evaluate the evolution of the gas density field.

6. Conclusion

A compact optical bench based on a RCRHI has been designed to analyze 2D unsteady wake flows. It uses three different wavelengths as luminous light sources and reflection panchromatic holographic plates. The best results are obtained when the diffraction efficiency of the plate is close to 50% for the three lines. For that, the gelatin shrinkage of Gentet and Slavich plates has to be mastered in order to avoid a variation in the gelatin thickness.

The wavelength coherence of the three lasers used has to be more than twice the distance between the hologram and the flat mirror located just behind the test section. Since the holographic plate is inserted between two collimated beams, the adjustment of the uniform background color or the choice of fringes is easier to obtain when the wind tunnel is running.

The interferogram analysis performed around the circular cylinder shows the large possibility of real-time three-color reflection holographic interferometry. But, with technological improvements performed in the area of matrix sensors, new perspectives in DCHI should be considered.

Concerning the analysis of the 3D flows, as the optical setup based on real-time three-color reflection holographic interferometry has been designed in one direction of view, our next work will consist of implementing an optical setup with three or four crossings of the test section.

References

1. J. M. Desse, F. Albe, and J. L. Tribillon, "Real-time color holographic interferometry," Appl. Opt. **41**, 5326–5333 (2002).
2. J. M. Desse, F. Albe, and J. L. Tribillon, "Real-time color holographic interferometry devoted to 2D unsteady wake flow," J. Visual. **7**, 217–224 (2004).
3. J. Surget, "Etude quantitative d'un écoulement aérodynamique," Rech. Aérosp. **3**, 167–171 (1973).
4. D. J. Cha and S. S. Cha, "Holographic interferometric tomography for limited data reconstruction," AIAA J. **34**, 1019–1026 (1996).
5. D. Yan and S. S. Cha, "Computational and interferometric system for real-time limited-view tomography of flow fields," Appl. Opt. **37**, 1159–1164 (1998).

6. N. Fomin, *Speckle Photography for Fluid Mechanics Measurements* (Springer, 1998).

7. N. Fomin, E. Lavinskaya, and D. Vitkin, "Speckle tomography of turbulent flows with density fluctuations," Exp. Fluids **33**, 160–169 (2002).

8. B. J. Pellicia-Kraft and D. W. Watt, "Three-dimensional imaging of a turbulent jet using shearing interferometry and optical tomography," Exp. Fluids **29**, 573–581 (2000).

9. B. J. Pellicia-Kraft and D. W. Watt, "Visualization of coherent structure in scalar fields of unsteady jet flows with interferometric tomography and proper orthogonal decomposition," Exp. Fluids **30**, 633–644 (2001).

10. B. Timmerman and D. W. Watt, "Tomographic high-speed digital holographic interferometry," Meas. Sci. Technol. **6**, 1270–1277 (1995).

11. L. Joannes, O. Dupont, F. Dubois, P. Colinet, and J. C. Legros, "Interferometric optical tomography for 3-dimensional investigation of liquids," in *Proceedings of the 8th International Symposium on Flow Visualization* (CD-ROM), G. M. Carlomagno, I. Grant, eds. (2000), paper 428.

12. G. E. A. Meier, "Computerized background-oriented Schlieren," Exp. Fluids **33**, 181–187 (2002).

13. G. Pedrini, W. Osten, and M. E. Gusev, "High-speed digital holographic interferometry for vibration measurement," Appl. Opt. **45**, 3456–3462 (2006).

14. C. Pérez-López, M. H. De la Torre-Ibarra, and F. M. Santoyo, "Very high speed cw digital holographic interferometry," Opt. Express **14**, 9709–9715 (2006).

15. I. Yamaguchi, T. Matsumura, and J. Kato, "Phase-shifting color digital holography," Opt. Lett. **27**, 1108–1110 (2002).

16. N. Demoli D. Vukicevic, and M. Torzynski, "Dynamic digital holographic interferometry with three wavelengths," Opt. Express **11**, 767–774 (2003).

17. J. M. Desse, P. Picart, and P. Tankam, "Digital three-color holographic interferometry for flow analysis," Opt. Express **16**, 5471–5480 (2008).

18. H. I. Bjelkhagen and E. Mirlis, "Color holography to produce highly realistic three-dimensional images," Appl. Opt. **47**, A123–A133 (2008).

19. Ts. Petrova, B. Ivanov, K. Zdravkov, D. Nazarova, E. Stoykova, G. Minchev, and V. Sainov, "Basic holographic characteristics of a panchromatic light sensitive material for reflective autostereoscopic 3D display," EURASIP J. Adv. Signal Process. **2009**, 1 (2009).

20. J. M. Desse, "Recent contribution in color interferometry and applications to high-speed flows," Opt. Lasers Eng. **44**, 304–320 (2006).

21. J. M. Desse, "Recording and processing of interferograms by spectral characterization of the interferometric setup," Exp. Fluids **23**, 265–271 (1997).